Available online at www.sciencedirect.com
ScienceDirect
International Journal of Heat and Mass Transfer 51 (2008) 4788–4796
International Journal of HEAT and MASS TRANSFER
www.elsevier.com/locate/ijhmt

Numerical study of pin-fin heat sink with un-uniform fin height design

Yue-Tzu Yang *, Huan-Sen Peng

Department of Mechanical Engineering, National Cheng Kung University, Tainan 70101, Taiwan

Received 27 August 2007; received in revised form 1 February 2008
Available online 8 April 2008

Abstract

This study presents the numerical simulation of the heat sink with an un-uniform fin height with a confined impingement cooling. The governing equations are discretized by using a control-volume-based finite-difference method with a power-law scheme on an orthogonal non-uniform staggered grid. The coupling of the velocity and the pressure terms of momentum equations are solved by the SIMPLEC algorithm. The well-known k–ε two-equations turbulence model is employed to describe the turbulent structure and behavior. The parameters include the Reynolds number ($Re = 15{,}000$ and $Re = 25{,}000$) and 12 un-uniform fin height designs (Type-b to Type-m). The objective of this study is to examine the effects of the fin shape of the heat sink on the thermal performance. It is found that the junction temperature can be reduced by increasing the fin height near the center of the heat sink. The results also show that there is a potential for optimizing the un-uniform fin height design.

Keywords: Pin-fin heat sink; Un-uniform fin height; Electronics cooling; CFD

1. Introduction

Since the rapid development of electronic technology, electronic appliances and devices now are always in our daily life. Under the condition of multifunction, high clock speed, shrinking package size, and higher power dissipations, the heat flux per unit area increased dramatically over the past few years. Besides, the working temperature of the electronic components may exceed the desired temperature level. Thus, the effective removal of heat dissipations and maintaining the die at a safe operating temperature have played an important role in insuring a reliable operation of electronic components.

There are many methods in electronics cooling, such as jet impingement cooling [1,2], heat pipe [3–5], etc. Conventional electronics cooling normally used impinging jet with heat sink showing superiority in terms of unit price, weight and reliability. Therefore, the most common way to enhance the air-cooling is through the utilization of impinging air jets on a heat sink. In order to design an effective heat sink, some criterions such as a large heat transfer rate, a low pressure drop, an easier manufacturing, a simpler structure, a reasonable cost and so on should be considered.

When the literature is surveyed, a number of scholars have examined the air-jet impingement on a heat sink in geometries, materials, and jet flow speed or nozzle target distance extensively. Ledezma et al. [6] performed an experimental, numerical and theoretical study of the heat transfer on a pin-finned plate. They carried out the correlation equations for optimal fin-to-fin spacing and the maximum thermal conductance. Brignoni and Garimella [7] performed the experimental optimization of confined impinging air jets used in conjunction with a pin-fin heat sink. Enhancement factors for the heat sink were evaluated, and the range of 2.8–9.7 was obtained relative to a bare surface. Average heat transfer coefficients and thermal resistance values were expressed for the heat sink as a

* Corresponding author. Tel.: +886 6 2757575x62172; fax: +886 6 2352973.
E-mail address: ytyang@mail.ncku.edu.tw (Y.-T. Yang).

0017-9310/$ - see front matter © 2008 Elsevier Ltd. All rights reserved.
doi:10.1016/j.ijheatmasstransfer.2008.02.017

Nomenclature

A_h	heating area (m^2)
b	thickness of the base of the heat sink (mm)
C_1, C_2, C_μ	turbulent constant
COE	coefficient of enhancement
d	diameter of the nozzle (m)
G	inter-fin spacing (mm)
h	heat transfer coefficient based on A_h (W/m^2 K)
H	height of the fins (mm)
k	turbulent kinetic energy (m^2/s^2)
k_a	thermal conductivity of air (W/m K)
k_s	thermal conductivity of aluminum alloy (W/m K)
L	length of the base of the heat sink (mm)
Nu	Nusselt number ($=hd/k_a$)
p	pressure (N/m^2)
Q	heating power (W)
Re	Reynolds number ($=\|V_{in}\|d/v$)
R_{th}	thermal resistance (°C/W)
T	temperature (°C)
u_i, u_j	velocity component (m/s)
V	velocity in the Y-direction (m/s)
W	width of the fins (mm)
x_i, x_j	coordinates (m)

Greek symbols

ΔT	junction to ambient temperature difference (°C)
ε	turbulent energy dissipation rate (m^2/s^2)
μ	dynamic viscosity (N s/m^2)
v	kinematic viscosity (m^2/s)
ρ	density (kg/m^3)
σ	Prandtl number
σ_k, σ_ε	turbulent constant

Subscripts

ave	average
base	base
film	film
in	inlet
l	laminar
new	new design
origin	original design
t	turbulent

function of a Reynolds number, an air flow rate, a pumping power, and a pressure drop, to assist in optimizing the jet impingement configuration for given design constraints. Maveety and Hendricks [8] showed the performance study of pin-fin heat sinks with impingement cooling which considered the effects of geometry, nozzle-to-heat sink vertical placement, material, and Reynolds number. The results revealed that the best performance occurred when the dimensionless impingement distance was between 8 and 12, and when the Reynolds number was between 40,000 and 50,000. The results also presented that due to the higher spreading resistance efficiency of the carbon composite material, it led to more uniform cooling of the heat sink. Moreover, the influence of the nozzle-to-heat sink vertical placement on the thermal performance was reduced as the Reynolds number increased. Maveety and Jung [9] have investigated the comparisons between computational and experimental results for the cooling performance from a pin-fin heat sink with an impinging air flow. Furthermore, optimization studies were discussed to quantify the effects of changing the fin length and the fin cross-sectional area on the cooling performance. The numerical results illustrated a complex pressure gradients inside the fin array and a greater pressure gradient improved mixing and heat transfer. Their simulations also demonstrated a complicated fluid motion with large pressure gradients that generated vorticity, circulation and flow reversals. The enhancement of heat transfer from a discrete heat source in a confined air jet impingement was experimentally studied by El-Sheikh and Garimella [10]. Relative to an unpinned heat sink, the heat transfer from the pinned ones was improved by 2.4–9.2 times. Due to the introduction of the heat sinks, the enhancement factors relative to the bare heat source varied from 7.5 to 72. Results for the average heat transfer coefficient were correlated as a function of the Reynolds number, fluid properties and geometric parameters of the heat sinks. An experimental study was conducted to investigate the heat transfer from a parallel flat plate heat sink under a turbulent air jet impingement by Sansoucy et al. [11]. The forced convection heat transfer rates from a flat plate and from a flat plated heat sink under an impinging confined jet have been obtained. In addition, the experimental results were compared with the numerical predictions obtained in an earlier study. They concluded that the numerical analysis in a previous study was adequate for appraising the mean heat transfer rate in jet impingement for situations of thermal management of electronics. Li et al. [12] and Li and Chen [13] investigated the thermal performance of pin-fin and plate-fin heat sinks with confined impingement cooling by using infrared thermography. The results show that the thermal resistance of the heat sinks decreases with the increased Reynolds number of the impinging jet. However, the reduction of the thermal resistance decreases gradually as the Reynolds number increases. Moreover, it revealed that the influence of fin width is more obviously than the fin height. In addition, the optimal impinging distance increases with increasing Reynolds number. Finally, they

concluded that the thermal performance of the pin-fin heat sinks is superior to that of the plate-fin heat ones. Furthermore, the thermal performance of pin-fin heat sinks with air impingement cooling was performed numerically and experimentally by Li and Chen [14]. The effects of the fin geometry and the Reynolds number on the heat transfer of the heat sinks were discussed, too. Duan and Muzychka [15] performed the experimental investigation of the thermal performance with four heat sinks of various impingement inlet widths, fin spacings, fin heights and airflow velocities. They developed a heat transfer model to predict the thermal performance of impingement air cooled plate fin heat sinks for design purposes. The thermal performance of a pin-fin heat sink was studied theoretically and experimentally by Kobus and Oshio [16]. They carried out a theoretical model that has the capability of predicting the influence of various physical, thermal and flow parameters on the effective thermal resistance of a pin-fin array heat sink. Besides, the predictive capability of the theoretical model was verified by comparing with experimental data and was shown to be exceptionally good over the range of parameters. The thermal and hydraulic behavior due to jet impingement on pin-fin heat sinks was experimentally investigated by Issa and Ortega [17]. This study showed that the pressure loss coefficient increased with increasing pin density and pin diameter, and decreased with increasing pin height and clearance ratio. Moreover, the overall base-to-ambient thermal resistance decreased with increasing Reynolds number, pin density and pin diameter. Kobus and Oshio [18] investigate the influence of thermal radiation on the thermal performance of a pin-fin array heat sink theoretically and experimentally. A theoretical thermal radiation model was developed for predicting the effective thermal resistance of a fin array heat sink.

Excluding numerical simulation or experimental studies, the entropy generation method was also utilized to evaluate or optimize the thermal performance of the heat sink [19–23]. The procedure is based on the minimization of entropy generation resulting from heat transfer and pressure drop. The model demonstrates a rapid, stable procedure for obtaining optimum design/operational conditions without resorting to parametric analysis by using repeated iterations with a thermal analysis tool.

Moreover, some scholars have interests in altering the fin shape to enhance the thermal and hydraulic performance. Lorenzini and Moretti [24] analyzed the Y-shape fins and examined the geometries by varying the angle between the two arms of the Y and proposed new shape for the fins. Ledezma and Bejan [25] performed the experimental and numerical study of heat sinks with sloped plate fins. This study discussed the thermal performance on the orientation of the fin array and the tilting of the crests of the plate fins. Sathe and Sammakia [26] have presented a study of a new and unique high-performance air-cooled impingement heat sink. The comparisons between numerical simulation and experimental data of the heat sink performance have been conducted. The effects of the fin thickness, inter-fin gap, nozzle width, and fin shape on the heat transfer and pressure drop have been studied. The study showed that the pressure drop can be decreased by cutting the fins in the central impingement zone without sacrificing heat transfer rates. Shah et al. [27] demonstrated the results of a numerical analysis of the performance of an impingement heat sink designed for use with a specific blower as a single unit. The effects of the shape of the heat sink fins, particularly near the center of the heat sink were examined. It is found that removal of fin material from the central region of the heat sink enhances the thermal as well as the hydraulic performance of the sink. Shah et al. [28] studied extends the previous work by investigating the effect of removal of a fin material from the end fins, the total number of fins, and the reduction in the size of the hub fan. The reduction in the size of the hub of the fan is found to be a more uniform distribution of the air inside the heat sink, particularly near the center of the module. Increasing the number of fins indicates a small drop in temperatures, accompanied by a significant pressure rise. Moreover, they reported a new optimal heat sink design by employing the actual fan operating characteristics.

In general, there are many testing processes for heat sinks which must be introduced in an effort to obtain the thermal and hydraulic performance of heat sinks. If we take advantage of the numerical simulation to obtain some probable optimal design parameters before running experiments, the cost and research time can be reduced. In this paper, the numerical simulation of pin-fin heat sinks with confined impingement cooling in thermal-fluid characteristics will be investigated. The objective of this study is to examine the effect of the un-uniform fin height design on the junction temperature and the thermal performance of the heat sink.

2. Mathematical model and numerical method

The schematic diagram of the geometry and the computational domain is shown in Fig. 1. The turbulent three-dimensional Navier–Stokes and energy equations are solved numerically (using finite-difference scheme) combined with the continuity equation to simulate the thermal and turbulent flow fields. An eddy viscosity model is used to account for the effects of turbulence. The flow is assumed to be steady, incompressible, and three-dimensional. The buoyancy and radiation heat transfer effects are neglect. In addition, the thermophysical properties of the fluid are assumed to be constant.

The three-dimensional governing equations of mass, momentum, turbulent kinetic energy, turbulent energy dissipation rate, and energy in the steady turbulent main flow using the standard k–ε model are as follows:

(1) Continuity equation

$$\frac{\partial \rho \bar{u}_i}{\partial x_i} = 0 \tag{1}$$

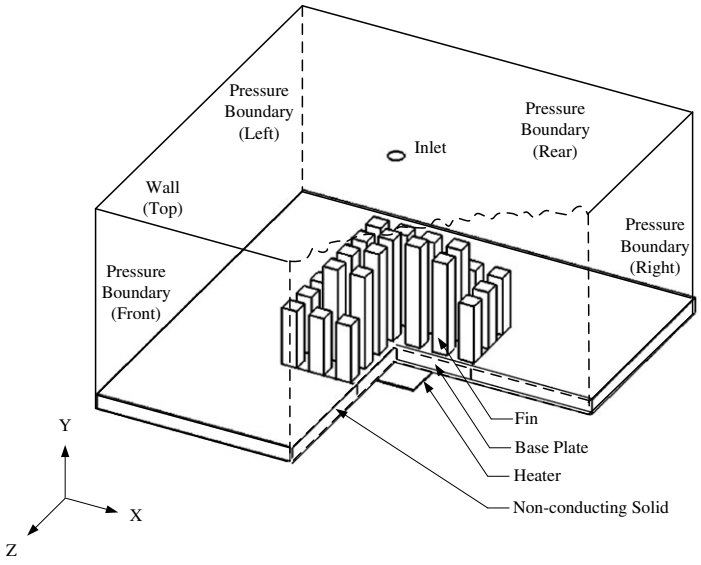

Fig. 1. Physical domain.

(2) Momentum equation

$$\rho\bar{u}_j\frac{\partial\bar{u}_i}{\partial x_j}=-\frac{\partial\bar{p}}{\partial x_i}+\frac{\partial}{\partial x_j}\left[\mu_t\left(\frac{\partial\bar{u}_i}{\partial x_j}+\frac{\partial\bar{u}_j}{\partial x_i}\right)\right] \tag{2}$$

(3) Energy equation

$$\rho\bar{u}_j\frac{\partial\bar{T}}{\partial x_j}=\frac{\partial}{\partial x_j}\left[\left(\frac{\mu_l}{\sigma_l}+\frac{\mu_t}{\sigma_t}\right)\frac{\partial\bar{T}}{\partial x_j}\right] \tag{3}$$

(4) Transport equation for k

$$\rho\bar{u}_j\frac{\partial k}{\partial x_j}=\frac{\partial}{\partial x_j}\left(\frac{\mu_t}{\sigma_k}\frac{\partial k}{\partial x_j}\right)+\mu_t\left(\frac{\partial\bar{u}_i}{\partial x_j}+\frac{\partial\bar{u}_j}{\partial x_i}\right)\frac{\partial\bar{u}_i}{\partial x_j}-\rho\varepsilon \tag{4}$$

(5) Transport equation for ε

$$\rho\bar{u}_j\frac{\partial\varepsilon}{\partial x_j}=\frac{\partial}{\partial x_j}\left(\frac{\mu_t}{\sigma_\varepsilon}\frac{\partial\varepsilon}{\partial x_j}\right)+C_1\mu_t\frac{\varepsilon}{k}\left(\frac{\partial\bar{u}_i}{\partial x_j}+\frac{\partial\bar{u}_j}{\partial x_i}\right)\frac{\partial\bar{u}_i}{\partial x_j}-C_2\rho\frac{\varepsilon^2}{k} \tag{5}$$

The empirical constants appear in the above equations are given by the following values: $C_1=1.44$, $C_2=1.92$, $C_\mu=0.09$, $\sigma_k=1.0$, $\sigma_\varepsilon=1.3$.

The governing equation for the solid can be written as

$$\frac{\partial}{\partial x_i}\left(k_s\frac{\partial T}{\partial x_i}\right)=0 \tag{6}$$

The Reynolds number of the impinging jet is defined as

$$Re=\frac{|V_{in}|d}{v} \tag{7}$$

where d denotes the diameter of nozzle.

The average convection heat transfer coefficient h is calculated by

$$h=\frac{Q}{A_h(T_{base}-T_{in})} \tag{8}$$

The average Nusselt number Nu is calculated by

$$Nu=\frac{hd}{k_a} \tag{9}$$

Following the definition given in Sansoucy et al. [11], the coefficient of enhancement (COE) is defined to quantify the improvement in heat transfer rates due to the difference types of the heat sink fins. This is expressed as

$$\mathrm{COE}=\frac{Nu_{new}}{Nu_{origin}} \tag{10}$$

where k_a is evaluated at the film temperature T_{film} $\left(T_{film}=\frac{T_{base}+T_{in}}{2}\right)$.

The thermal resistance of the heat sink is calculated by

$$R_{th}=\frac{T_{ave}-T_{in}}{Q} \tag{11}$$

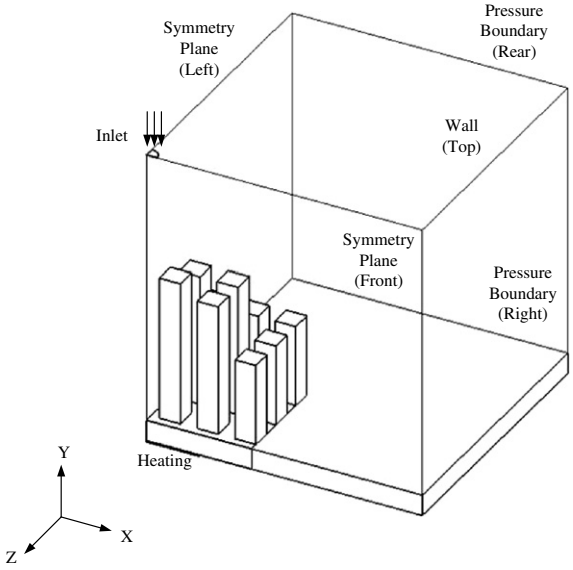

Fig. 2. Computational domain and boundary conditions.

The dimensions of the computational domain were based on the work by Li and Chen [14]. Taking advantage of the symmetry, the numerical simulations have been performed by considering only a one-quarter model of the physical domain. The boundary conditions for this problem are stated as follows: at the flow inlet, the air was uniformly induced downward with a constant temperature. The pressure boundary conditions are used at the outlet. No slip conditions with thermally insulated are provided on all the other confined walls. At the bottom of the heat sink, an uniform constant heat flux is applied on the heating area. The adiabatic thermal boundary conditions are utilized at the outer perimeter of the bottom of heat sink except for the heating area. In addition, because of symmetric assumptions only a quarter of a heat sink and a quarter of channel are calculated as shown in Fig. 2.

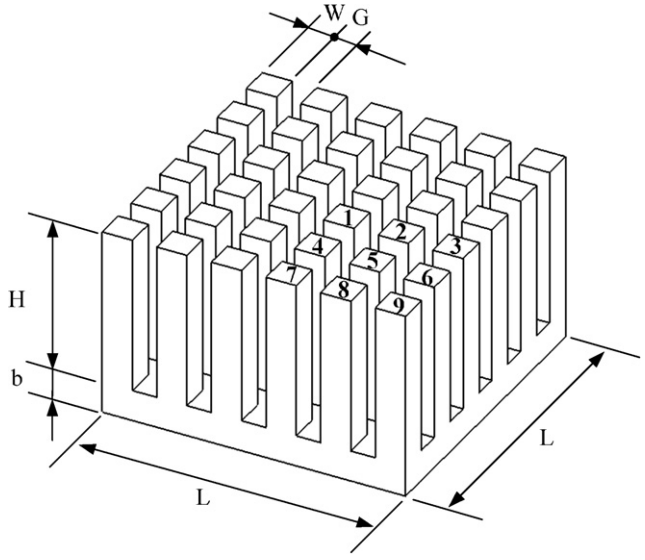

Fig. 3. Geometry of heat sink (original design).

A non-uniform and staggered grid system with a large concentration of nodes in regions of steep gradients, such as those close to the walls was employed. A staggered grid arrangement is used in which the velocities are stored at a location on the control-volume faces. All other variables including pressure are calculated at the grid points. The numerical method used in the present study is base on the SIMPLEC (semi-implicit method for pressure-linked equation consistent) algorithm of Doormaal and Raithby [29]. Pressure and velocity correction schemes are implemented in the model algorithm to arrive at a converged solution when both the pressure and velocity satisfy the momentum and continuity equations. For non-linear problems, under-relaxation is employed to avoid divergence in the iterative solutions. The resulting sets of discretized equations for each variable are solved by the line-by-line procedure which is the combination of the tri-diagonal matrix algorithm (TDMA) and the Gauss–Seidel iteration technique of Patankar [30]. The solution is considered to be converged when the normalized residual of the algebraic equation is less than a prescribed value of 10^{-3}.

3. Results and discussion

The denotations and dimensions of the aluminum pin-fin heat sinks with different un-uniform fin height designs in this study are depicted in Fig. 3 and Table 1. In Table 1, the geometric parameters of Type-a are the same as the one of the Li and Chen's [14] studies. And the designs from Type-b to Type-m are extended from the Type-a. The effects of the Reynolds number and the un-uniform fin height design on the junction temperature and thermal performance are examined. The parameters used in this study include two Reynolds numbers ($Re = 15{,}000$ and $Re = 25{,}000$) and 12 un-uniform fin height designs (Type-b to Type-m). And the constraint on the un-uniform fin height design is in the same volume with the original

Table 1
Dimensions of the fins

Group	Fin shape	H (mm)								
		Fin-1	Fin-2	Fin-3	Fin-4	Fin-5	Fin-6	Fin-7	Fin-8	Fin-9
	Type-a	40	40	40	40	40	40	40	40	40
I	Type-b	50	50	40	50	40	30	40	30	30
	Type-c	55	55	40	55	40	25	40	25	25
	Type-d	60	60	40	60	40	20	40	20	20
II	Type-e	45	45	45	45	45	30	45	30	30
	Type-f	50	50	50	50	50	20	50	20	20
	Type-g	55	55	55	55	55	10	55	10	10
III	Type-h	50	50	35	50	35	35	35	35	35
	Type-i	54	54	33	54	33	33	33	33	33
	Type-j	60	60	30	60	30	30	30	30	30
IV	Type-k	50	45	35	45	45	35	35	35	35
	Type-l	55	50	31	50	50	31	31	31	31
	Type-m	60	50	30	50	50	30	30	30	30

$L = 80$ mm, $b = 8.0$ mm, $W = 8.0$ mm

design. Moreover, we classify these 12 designs into four groups and compare with the original design. Fig. 4 shows the configuration of the four groups of the heat sinks. The material of heat sink is selected as aluminum alloy 6061 and has a value 168 W/m K in thermal conductivity. Both of the length and width of the base of the heat sink are 80 mm. The area of the heater is 40 mm × 40 mm, which is in the center of the heat sink. And the heating area is heated with heating power 100 W.

3.1. Verification

In order to verify the present numerical model, the thermal resistance under the conditions $Re = 5000$–$25{,}000$ and $Q = 20$ W with the uniform fin height ($H = 40$ mm) are compared with Li and Chen [14] as shown in Fig. 5. Moreover, a total number of meshes, 69,815, 98,795 and 137,624 were employed to assess the grid independence. The results of the grid sensitivity study showed that the simulations based on the 98,795 meshes provide satisfactory numerical accuracy. The average error between simulation results and experimental data is about 16.4%. Reasonable discrepancies between numerical calculations and the available experimental results of Li and Chen [14] may be caused by the isotropic assumption, numerical error or 9.1% uncertainty of Li and Chen [14].

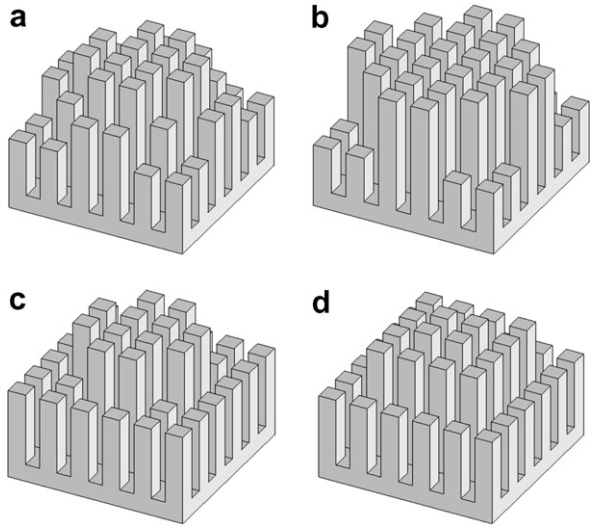

Fig. 4. Schematic diagram showing different un-uniform fin height design in the study: (a) group-I, (b) group-II, (c) group-III and (d) group-IV.

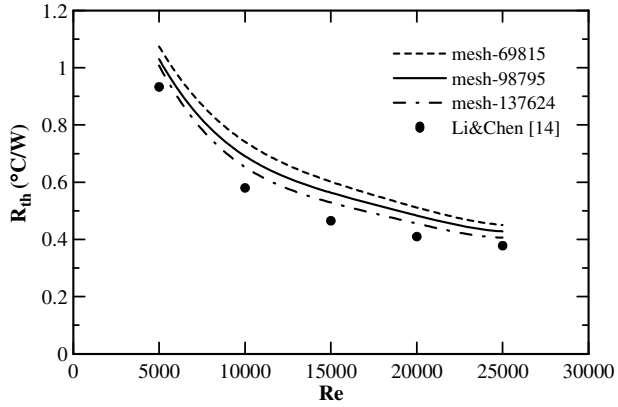

Fig. 5. Comparison between numerical and experimental values of the thermal resistance.

3.2. Fin shape study

Fig. 6 shows the trend of thermal performance for the group-I. As seen in this figure, the temperature difference decreases as the fin shape changes from Type-a to Type-b. And the difference in COE between the original design (Type-a) and Type-b appeared to be minimal. When the

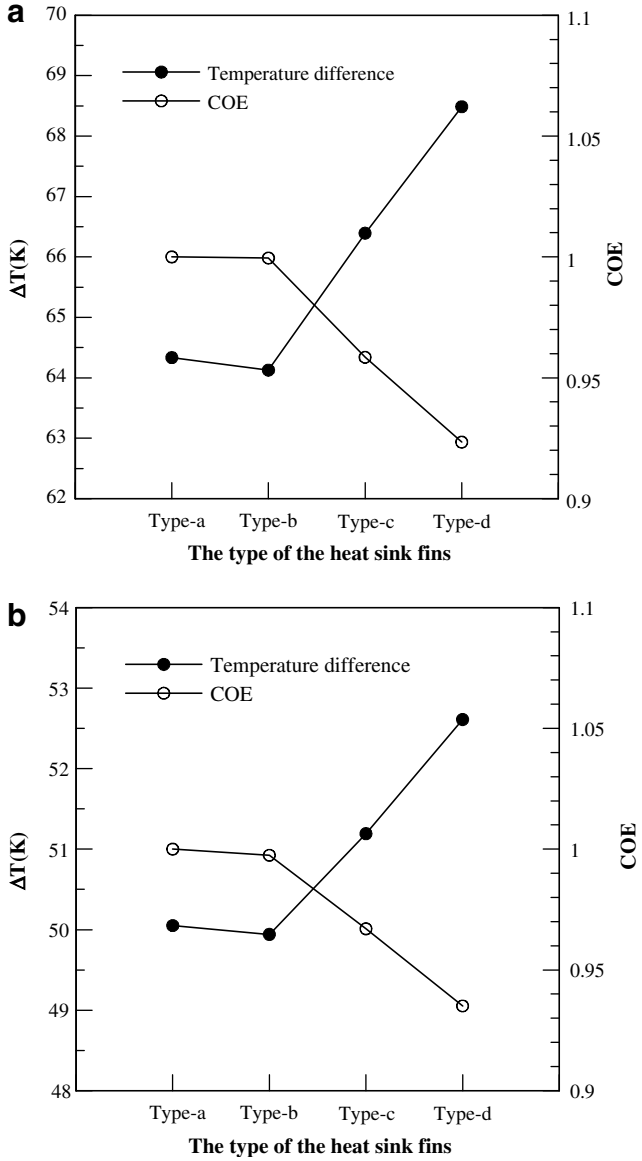

Fig. 6. Trend of thermal performance for group-I: (a) $Re = 15{,}000$ and (b) $Re = 25{,}000$.

fin shape changes from Type-b to Type-c, the temperature difference dramatically increases and the COE decreases. The increment of temperature difference between the original design and Type-c is 2.06 K at $Re = 15{,}000$ and 1.14 K at $Re = 25{,}000$. And Type-c results in a COE that is 4.2% lower than the original design at $Re = 15{,}000$ and 3.3% at $Re = 25{,}000$. When the fin shape changes from Type-c to Type-d, the trends of the temperature difference and the COE are similar to the previous. In group-I, Type-b is the good practical choice.

Fig. 7 depicts the trend of thermal performance for the group-II. This figure shows that the temperature difference increases when the fin shape changes from Type-a to Type-e. And the COE decreases as the temperature difference increases. When the fin shape changes from Type-e to Type-f, the trends of the temperature difference and the COE are similar to the previous case. As the fin shape changes from Type-a to Type-g, the temperature difference increases from 64.33 K to 67.91 K at $Re = 15{,}000$ and 50.05 K to 51.88 K at $Re = 25{,}000$. The reduction of the COE obvious increase is due to the dramatic increase of the temperature difference. As seen in Fig. 7, the thermal performances of the group-II are not good.

The trend of thermal performance for group-III is shown in Fig. 8. It can be seen that the temperature difference decreases from 64.33 K to 63.96 K at $Re = 15{,}000$ and 50.05 K to 49.45 K at $Re = 25{,}000$ when the fin shape changes from Type-a to Type-h. The COE increases with the decreasing temperature difference. When the fin shape changes from Type-a to Type-i, the temperature difference increases and the COE decreases at $Re = 15{,}000$. But at $Re = 25{,}000$, the temperature difference decreases, and the COE appeared to decrease at a small amount. As the fin shape design is Type-j, the temperature difference rises

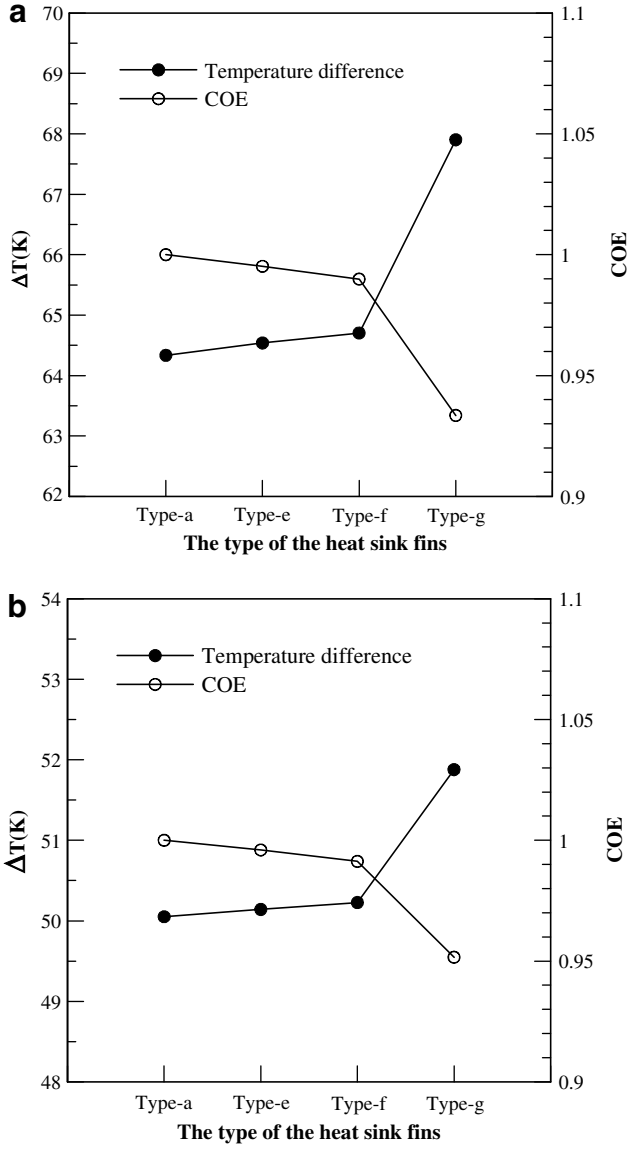

Fig. 7. Trend of thermal performance for group-II: (a) $Re = 15{,}000$ and (b) $Re = 25{,}000$.

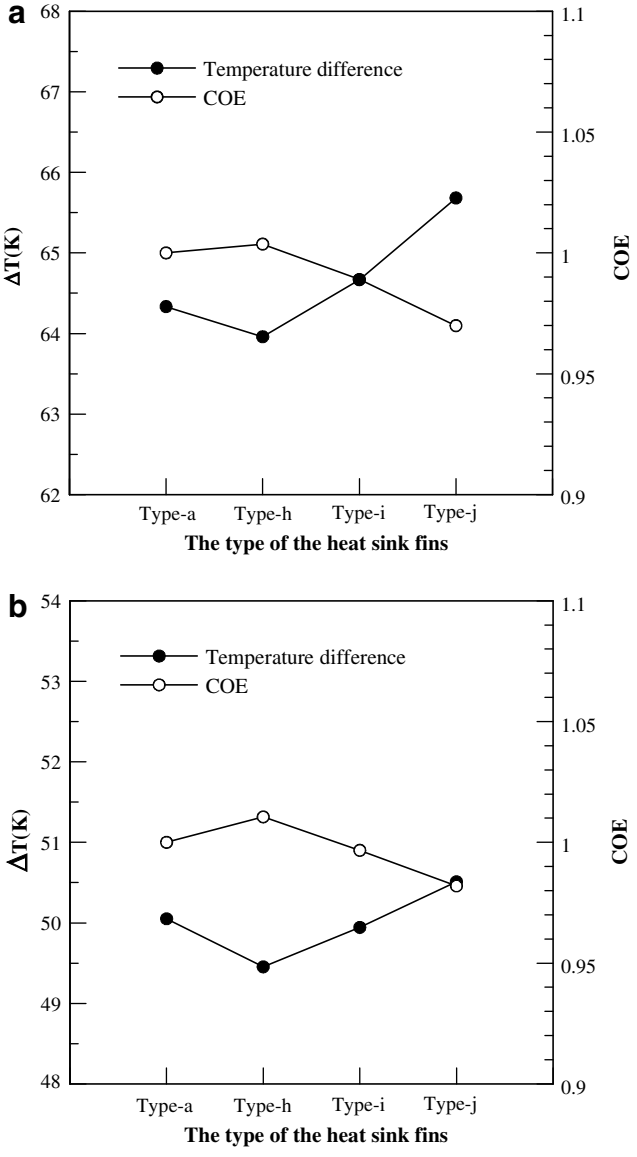

Fig. 8. Trend of thermal performance for group-III: (a) $Re = 15{,}000$ and (b) $Re = 25{,}000$.

to 65.68 K at $Re = 15{,}000$ and 50.51 K at $Re = 25{,}000$. And as usual, the COE decreases with the increasing temperature difference. In this group, Type-h is superior to the other designs.

Fig. 9 shows the trend of thermal performance for group-IV. When the fin shape changes from Type-a to Type-k, the temperature difference decreases and the COE increases simultaneously. As the fin shape design is Type-l or Type-m, the temperature difference increases and the COE decreases. As the figures indicate, Type-k is the better choice in this group.

Generally speaking, the COE increases as the temperature difference decreases. The effects of the fin design are more obviously at low Reynolds numbers. The junction temperature can be reduced by increasing the fin height near the center of the heat sink. It improves the thermal performance simultaneously. But it has a limitation on increasing the fin height near the center of the heat sink. The flow penetration into the center of the heat sink becomes weaker due to the increased flow resistance. Hence, the junction temperature will be increased. Furthermore, if the fins near the center of the heat sink increase excessively, the other fins will be too short. It makes the poor heat dissipation by the side of the heat sink and reduces the whole thermal performance.

3.3. A comprehensive comparison

Fig. 10 depicts the effect of the different fin shape designs on the thermal performance. As shown in Fig. 10a, the temperature difference of Type-k and Type-h is lower than that of the original design, and the COE is higher than that of the original design. These two design are better than the original ones at $Re = 15{,}000$. At $Re = 25{,}000$, as seen in

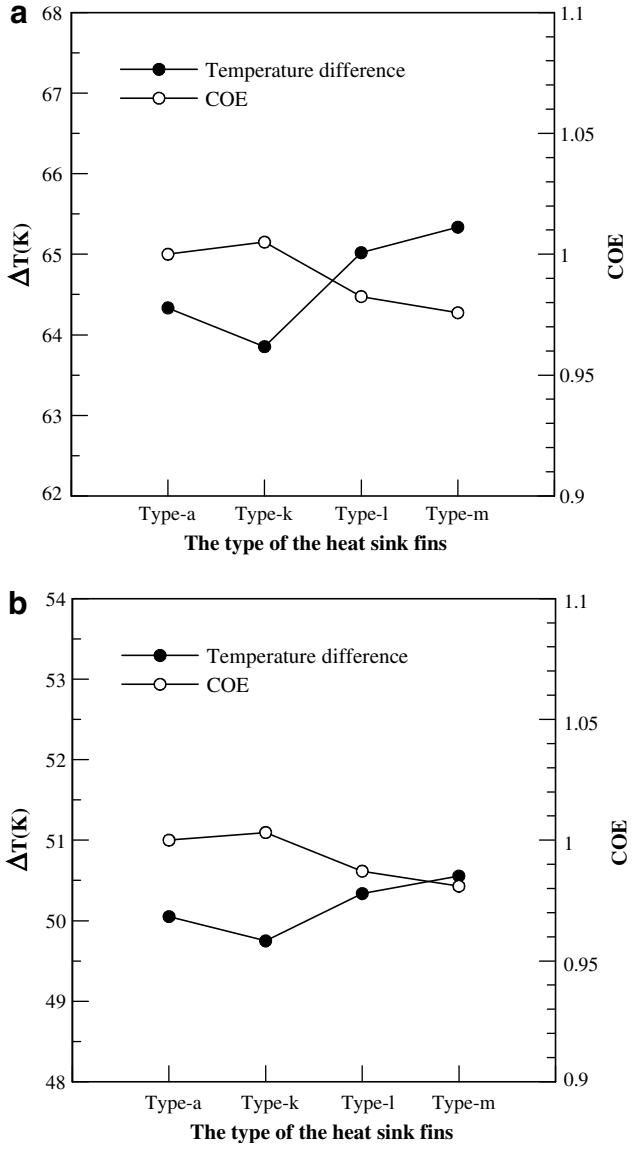

Fig. 9. Trend of thermal performance for group-IV: (a) $Re = 15{,}000$ and (b) $Re = 25{,}000$.

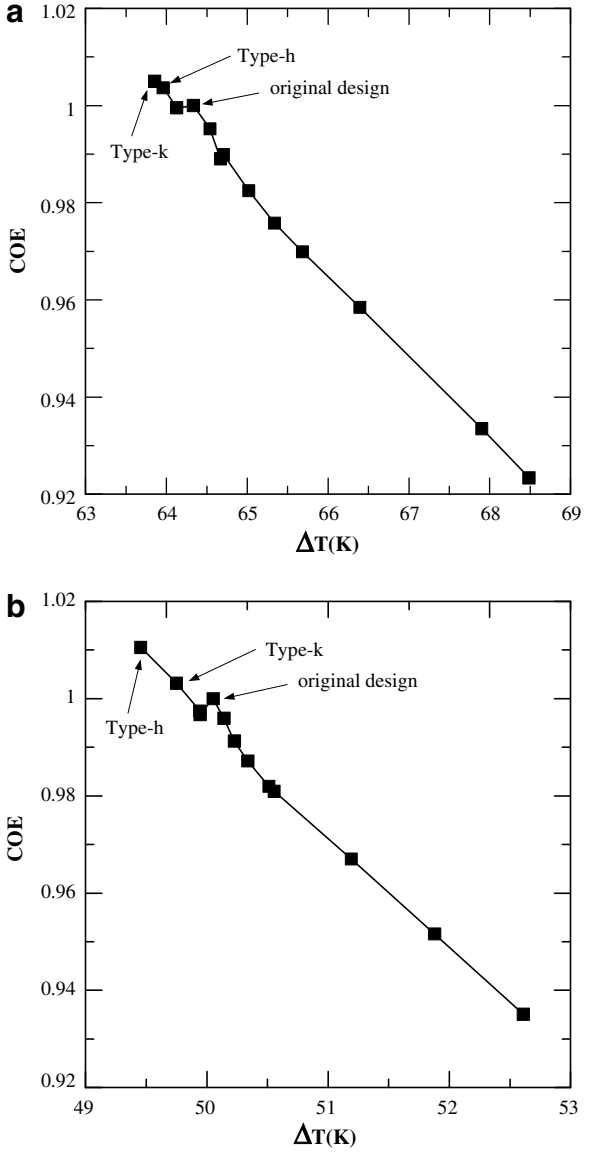

Fig. 10. Variation of COE as a function of temperature difference: (a) $Re = 15{,}000$ and (b) $Re = 25{,}000$.

Fig. 10b, Type-h and Type-k are still the better designs than the original ones. Although the influences of design parameters of heat sink considered for comparison of the temperature difference and the COE of heat sink are not so significant, the numerical approach has proven for the evaluation of performance.

4. Conclusion

The numerical simulation of pin-fin heat sinks with confined impingement cooling at various Reynolds numbers and un-uniform fin height designs are proposed. The purpose of this study is to evaluate the possibility of improving the heat sink performance by minimizing the junction temperature of the heat sink without sacrificing the whole thermal performance. It is found that an adequate un-uniform fin height design could decrease the junction temperature and increase the enhancement of the thermal performance simultaneously. The results also show that there is a potential for optimizing the un-uniform fin height design.

Acknowledgements

The support of the National Science Council (NSC) of Taiwan under contract no. NSC 96-2221-E-006-161-MY2 is gratefully acknowledged. The authors also want to thank the National Center for High-Performance Computing (NCHC) for providing computer resources.

References

[1] Y.M. Chung, K.H. Luo, Unsteady heat transfer analysis of an impinging jet, J. Heat Transfer 124 (2002) 1039–1048.
[2] K. Nishino, M. Samada, K. Kasuya, K. Torii, Turbulence statistics in the stagnation region of an axisymmetric impinging jet flow, Int. J. Heat Fluid Flow 17 (1996) 193–201.
[3] K.S. Kim, M.H. Won, J.W. Kim, B.J. Back, Heat pipe cooling technology for desktop PC CPU, Appl. Thermal Eng. 23 (2003) 1137–1144.
[4] Y. Wang, K. Vafai, An experimental investigation of the thermal performance of an asymmetrical flat plate heat pipe, Int. J. Heat Mass Transfer 43 (2000) 2657–2668.
[5] Z. Zhao, C.T. Avedisian, Enhancing forced air convection heat transfer from an array of parallel plate fins using a heat pipe, Int. J. Heat Mass Transfer 40 (13) (1997) 3135–3147.
[6] G. Ledezma, A.M. Morega, A. Bejan, Optimal spacing between pin fins with impinging flow, J. Heat Transfer 118 (1996) 570–577.
[7] L.A. Brignoni, S.V. Garimella, Experimental optimization of confined air jet impingement on a pin fin heat sink, IEEE Trans. Compon. Packag. Technol. 22 (3) (1999) 399–404.
[8] J.G. Maveety, J.F. Hendricks, A heat sink performance study considering material, geometry, reynolds number with air impingement, J. Electron. Packag. 121 (1999) 156–161.
[9] J.G. Maveety, H.H. Jung, Design of an optimal pin-fin heat sink with air impingement cooling, Int. Commun. Heat Mass Transfer 27 (2) (2000) 229–240.
[10] H.A. El-Sheikh, S.V. Garimella, Enhancement of air jet impinging heat transfer using pin-fin heat sinks, IEEE Trans. Compon. Packag. Technol. 23 (2) (2000) 300–308.
[11] E. Sansoucy, P.H. Oosthuizen, G.R. Ahmed, An experimental study of the enhancement of air-cooling limits for telecom/datacom heat sink applications using an impinging air jet, J. Electron. Packag. 128 (2006) 166–171.
[12] H.Y. Li, S.M. Chao, G.L. Tsai, Thermal performance measurement of heat sinks with confined impinging jet by infrared thermography, Int. J. Heat Mass Transfer 48 (2005) 5386–5394.
[13] H.Y. Li, K.Y. Chen, Thermal performance of plate-fin heat sinks under confined impinging jet conditions, Int. J. Heat Mass Transfer 50 (2007) 1963–1970.
[14] H.Y. Li, K.Y. Chen, Thermal-fluid characteristics of pin-fin heat sinks cooled by impinging jet, J. Enhan. Heat Transfer 12 (2) (2005) 189–201.
[15] Z. Duan, Y.S. Muzychka, Experimental investigation of heat transfer in impingement air cooled plate fin heat sinks, J. Electron. Packag. 128 (2006) 412–418.
[16] C.J. Kobus, T. Oshio, Development of a theoretical model for predicting the thermal performance characteristics of a vertical pin-fin array heat sink under combined forced and natural convection, Int. J. Heat Mass Transfer 48 (2005) 1053–1063.
[17] J.S. Issa, A. Ortega, Experimental measurements of the flow and heat transfer of a square jet impinging on an array of square pin fins, J. Electron. Packag. 128 (2006) 61–70.
[18] C.J. Kobus, T. Oshio, Predicting the thermal performance characteristics of staggered vertical pin fin array heat sinks under combined mode radiation and mixed convection with impinging flow, Int. J. Heat Mass Transfer 48 (2005) 2684–2696.
[19] J.R. Culham, Y.S. Muzychka, Optimization of plate fin heat sinks using entropy generation minimization, IEEE Trans. Compon. Packag. Technol. 24 (2) (2001) 159–165.
[20] W.W. Lin, D.J. Lee, Second-law analysis on a flat plate-fin array under crossflow, Int. Commun. Heat Mass Transfer 27 (2) (2000) 179–190.
[21] S.Z. Shuja, S.M. Zubair, M.S. Khan, Thermoeconomic design and analysis of constant cross-sectional area fins, Heat Mass Transfer 34 (1999) 357–364.
[22] W.A. Khan, J.R. Culham, M.M. Yovanovich, Optimization of pin-fin heat sinks using entropy generation minimization, ITHERM 1 (August) (2004) 259–267.
[23] K. Ogiso, Assessment of overall cooling performance in thermal design of electronics based on thermodynamics, J. Heat Transfer 123 (2001) 999–1005.
[24] G. Lorenzini, S. Moretti, Numerical analysis on heat removal from Y-shaped fins: efficiency and volume occupied for a new approach to performance optimisation, Int. J. Thermal Sci. 46 (2007) 573–579.
[25] G. Ledezma, A. Bejan, Heat sinks with sloped plate fins in natural and forced convection, Int. J. Heat Mass Transfer 39 (9) (1996) 1773–1783.
[26] S.B. Sathe, B.G. Sammakia, An analytical study of the optimized performance of an impingement heat sink, J. Electron. Packag. 126 (2004) 528–534.
[27] A. Shah, B.G. Sammakia, H. Srihari, K. Ramakrishna, A numerical study of the thermal performance of an impingement heat sink-fin shape optimization, IEEE Trans. Compon. Packag. Technol. 27 (4) (2004) 710–717.
[28] A. Shah, B.G. Sammakia, K. Srihari, K. Ramakrishna, Optimization study for a parallel plate impingement heat sink, J. Electron. Packag. 128 (2006) 311–318.
[29] J.P. van Doormaal, F.D. Raithby, Enhancements of the SIMPLE method for predicting incompressible fluid flows, Numer. Heat Transfer 7 (1984) 147–163.
[30] S.V. Patankar, Numerical Heat Transfer and Fluid Flow, McGraw-Hill, New York, 1980.